Investigation of the anomalously low $B(E2; 4_1^+ \rightarrow 2_1^+)/B(E2; 2_1^+ \rightarrow 0_1^+)$ ratio in ^{134}Ce through lifetime measurements

B. J. Zhu (朱保吉),[1] C. B. Li (李聪博),[1,*] X. G. Wu (吴晓光),[1,†] J. Zhong (钟健),[1] Q. M. Chen (陈启明),[1] Y. Zheng (郑云),[1] C. Y. He (贺创业),[1] W. K. Zhou (周文奎),[1] L. T. Deng (邓利涛),[1,2] and G. S. Li (李广生)[1]

[1]*China Institute of Atomic Energy, Beijing 102413, China*

[2]*College of Physics and Technology, Shenzhen University, Shenzhen 518060, China*

(Received 26 September 2016; published 9 January 2017)

The existing experimental value of the ratio $B_{4/2} \equiv B(E2; 4_1^+ \rightarrow 2_1^+)/B(E2; 2_1^+ \rightarrow 0_1^+)$ in ^{134}Ce is less than unity, which is outside the range allowed by current collective models and is highly anomalous. In the present work, new lifetime measurements of excited states in ^{134}Ce have been performed in order to clarify this discrepancy. Excited states of ^{134}Ce were populated by the fusion-evaporation reaction ^{122}Sn(^{16}O,$4n$)^{134}Ce. The recoil distance doppler shift method was employed, and reliable lifetimes for the 2_1^+, 4_1^+, 10_2^+, and 12_2^+ states were derived from the differential decay curve method. The resulting $B_{4/2}$ value is larger than unity, resolving the disagreement with traditional collective models. The new experimental data is in very good agreement with the calculation in the framework of the interacting boson model. The systematic evolution in collectivity of the Ce isotopes is discussed.

DOI: 10.1103/PhysRevC.95.014308

I. INTRODUCTION

Experimental determinations of electromagnetic transition rates give particularly valuable insights into the nature of nuclear collectivity, and they are crucial quantities for testing nuclear models. For spherical, near magic nuclei the transition probability $B(E2; 2_1^+ \rightarrow 0_1^+)$ value in W.u. is very low ($\sim$ a few W.u.), vibrational nuclei have on the order of tens of W.u., while $B(E2; 2_1^+ \rightarrow 0_1^+)$ values are very large for well-deformed nuclei. In standard collective models, a universal feature is that the $E2$ transition strengths of the 4^+ state is larger than the 2^+ state, accordingly $B_{4/2} \equiv B(E2; 4_1^+ \rightarrow 2_1^+)/B(E2; 2_1^+ \rightarrow 0_1^+) > 1$. The $B_{4/2}$ ratio is smaller than 1, which is extremely rare for collective nuclei and inconsistent with model predictions. Generally, such ratios are possible in around closed shells where the number of unpaired nucleons, seniority, is a good quantum number [1]. A systematics of these ratios of all even-even nuclei for medium and heavy mass nuclei with Z from 40 to 80 (except $N = 50$ and 82) pointed out a small set of nine nonmagic nuclei with anomalous values of the $B(E2)$ ratio $B_{4/2} < 1$ [2]. In these nine nuclei, each $B(E2; 2_1^+ \rightarrow 0_1^+)$ value is larger than 10 W.u., indicating collective nature, in contrast to that suggested by their $B_{4/2}$ values, which contradicts the predictions of collective models. Such discrepancies in ^{98}Ru and ^{180}Pt have turned out to be due to flawed measurements [3,4]. Additional remeasured $B_{4/2}$ values for ^{114}Te and ^{144}Nd [5,6], which only have two nucleons outside the $Z = 50$ or $N = 82$ closed shell, confirmed the anomaly, which has been discussed in terms of the interplay of collective and single-particle degrees of freedom. Hence, further measurements for remaining nuclei should be performed to ensure that the reported $B_{4/2}$ values are correct; only then can a full evaluation be made of the status of this anomalous behavior.

^{134}Ce, with $B_{4/2} = 0.79(15)$, is one of the anomalous nuclei in Ref. [2]. However, unlike ^{114}Te and ^{144}Nd, this nucleus is nonmagic and far away from both neutron and proton shell closures, despite the fact that it contains a large number of valence nucleons and therefore would normally be considered to be a collective nucleus with large $B_{4/2}$ value. Moreover, with the excitation energy ratio $R_{4/2} \equiv E(4_1^+)/E(2_1^+) = 2.56$, one could anticipate the collectivity of this nucleus to be in the transitional region between well-deformed and single-particle regimes. If this anomalous low $B_{4/2}$ is true, it is a significant structural puzzle that defies traditional models. However, past relevant lifetimes were measured in singles experiments [7] in which it is now well known that effects of level lifetimes involved in side-feeding transitions very probably give erroneous results. Thus, in the present work, the excited lifetimes of ^{134}Ce were remeasured by means of the recoil distance Doppler shift (RDDS) [8,9] technique to clarify the situation of the anomalous $B_{4/2}$ value. The data were collected in the γ-γ coincidence mode rather than the customary singles mode in order to reduce the complexities of the γ-ray spectra and to avoid some of the problems associated with side feeding to excited states. Lifetimes were determined by analyzing the transitions in coincidence mode, employing the differential decay curve method (DDCM) [10,11].

II. EXPERIMENTAL SETUP

The excited states of ^{134}Ce were populated using the fusion evaporation reaction ^{122}Sn(^{16}O,$4n$)^{134}Ce at an incident energy of 76 MeV. The ^{16}O beam was delivered by the HI-13 tandem accelerator at the China Institute of Atomic Energy (CIAE). The beam current was limited to 2 p nA in the process of whole experiment. The target consisted of 800 μg/cm^2 ^{122}Sn evaporated on a 1.9 mg/cm^2 ^{181}Ta foil facing the beam. A 9.9 mg/cm^2 tantalum foil was used to stop the ^{134}Ce recoil

*Corresponding author: licb@ciae.ac.cn
†Corresponding author: wxg@ciae.ac.cn

nuclei, which left the target with a mean velocity of 0.92% of the velocity of light, c. The target and stopper foils were mounted in the CIAE plunger. In this apparatus, the target-to-stopper distance is changed by moving the target. In order to compensate for variations due to the heating caused by the beam, the plunger system uses an automatic feedback system. The capacitance between the two foils was monitored in real time, and once the deviation between the distance exceeded 0.3 μm, the feedback system was activated to compensate for the distance change in the range 0–200 μm. Sudden changes in the target-to-stopper separation (or the capacitance) caused by beam heating and by mechanical vibrations were not found. More details about the CIAE plunger setup can be found in Ref. [12]. Eight target-to-stopper distances of 4, 8, 15, 28, 54, 104, 200, and 380 μm were used to record RDDS data, and longer periods of beam time were spent on shorter distances in order to be sensitive to shorter lifetimes.

Prompt γ rays were detected by an array comprising 10 Compton-suppressed high-purity germanium (HPGe) detectors. For the final RDDS analysis only seven of the detectors, four at an angle of 153° and three at an angle of 42° with respect to the beam line, could be used due to their suitable angular positions. Spectra for the analysis of the RDDS data were obtained by setting a gate from above, on the shifted component of a transition feeding directly the level of interest. Figure 1 shows the examples of spectra taken at different distances for the $2_1^+ \rightarrow 0_1^+$ transition at 409.1 keV and the $4_1^+ \rightarrow 2_1^+$ transition at 639.7 keV in ^{134}Ce.

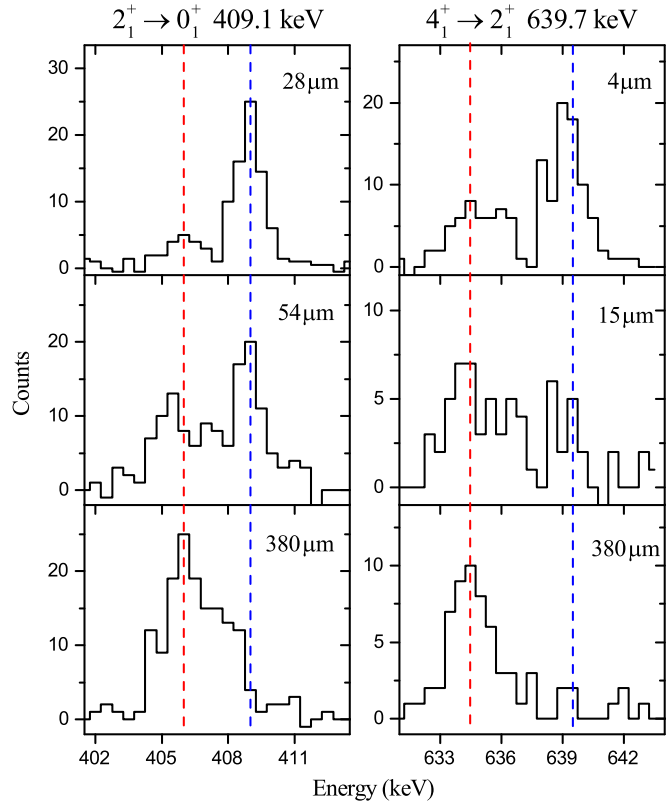

FIG. 1. Gated γ-ray spectra of ^{134}Ce taken at different distances. On the left-hand side, the shifted and unshifted components of the $2_1^+ \rightarrow 0_1^+$ transition are presented; on the right-hand side, the shifted and unshifted components of the $4_1^+ \rightarrow 2_1^+$ transition are shown. In these spectra the shifted component lies lower in energy ($\theta = 153°$) than the unshifted component.

III. DATA ANALYSIS AND RESULTS

In order to determine lifetimes of the investigated levels, the DDCM method was used in coincidence mode, and the uncertainties that result from the complicated side-feeding mechanism of the ground states were excluded. From the spectra gated on the shifted components of directly feeding γ transitions we obtained the peak intensities of γ transitions depopulating the level of interest at different target-to-stopper distances x. The peak intensities acquired at different target-to-stopper distances were normalized by generating spectra with gates set on both the shifted and unshifted components of the $4_1^+ \rightarrow 2_1^+$ transition. Then the summed intensities of the shifted and unshifted components of the higher lying transitions $6_1^+ \rightarrow 4_1^+$ and $8_1^+ \rightarrow 6_1^+$ were determined. The final lifetimes were extracted from an average of values determined at specific target-to-stopper distances using

$$\tau(x) = \frac{\{B_s, A_u\}(x)}{\frac{d}{dx}\{B_s, A_s\}(x)} \frac{1}{v}, \quad (1)$$

where v denotes the recoil velocity. The quantities $\{B_s, A_u\}(x)$ and $\{B_s, A_s\}(x)$ denote the measured intensities of the depopulating γ transition A in coincidence with the shifted component of a populating γ transition B. The derivative, $\frac{d}{dx}\{B_s, A_s\}(x)$, was determined by fitting piecewise continuously differentiable second-order polynomials to the intensity values. In the ideal case, the derived values of $\tau(x)$ should not depend on the distance at which they have been determined and correspondingly should be constant curves when plotted versus distance. Thus several independent lifetime values for a given level can provide a consistency check of the results, and a deviation from such behavior immediately indicates the presence of systematic errors in the analysis. A detailed description of this method is given in Refs. [10,11].

For the lifetime analysis of low-spin states in the ground-state band of ^{134}Ce with the reaction used, one has to deal with the problem that the majority of the feeding of the ground-state band is from long-lived states. For reference, Fig. 2 gives a partial level scheme for ^{134}Ce relevant to the present discussion. It should be noted that the lifetimes of 5^- states in neighboring isotopes ^{136}Ce [15] and ^{138}Ce [16] have been measured with $\tau = 716$ ps and $\tau = 650$ ps respectively. It is the same situation in ^{134}Ce, in which for the 1125.2 keV γ peaks, depopulating from the level of 5^- state at 2174.0 keV, only a fraction of Doppler-shifted intensity can be found even at a largest target-to-stopper distance (380 μm in this experiment, which corresponds to a time of flight of 138 ps of the recoiling nuclei), indicating a rather long lifetime. The 4_1^+ state of the ground-state band is fed directly from this 5^- level, whereas the 8_1^+ state is fed from the 10_1^+ level at 3207.9 keV and the 10_2^+ level at 3718.9 keV with lifetimes of 444 ns [17] and 9.6 ps (the determination of the 10_2^+ state lifetime via the DDCM will be described below), respectively. The longest feeding time into the ground-state band originates from the 396.8 keV transition

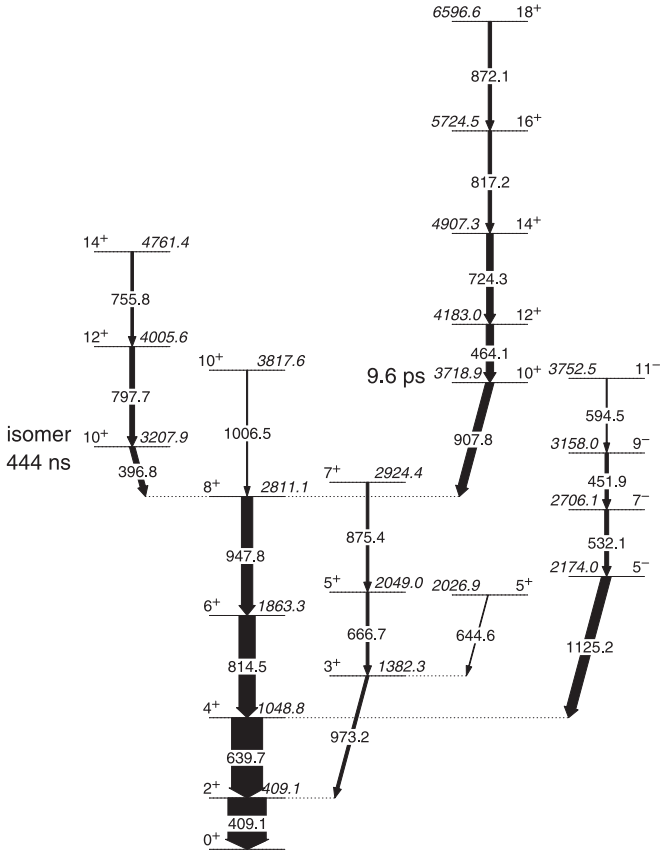

FIG. 2. Partial level scheme showing the main feeding transitions into the ground-state band according to Refs. [13,14]. The widths of the arrows correspond to the intensities of each transition.

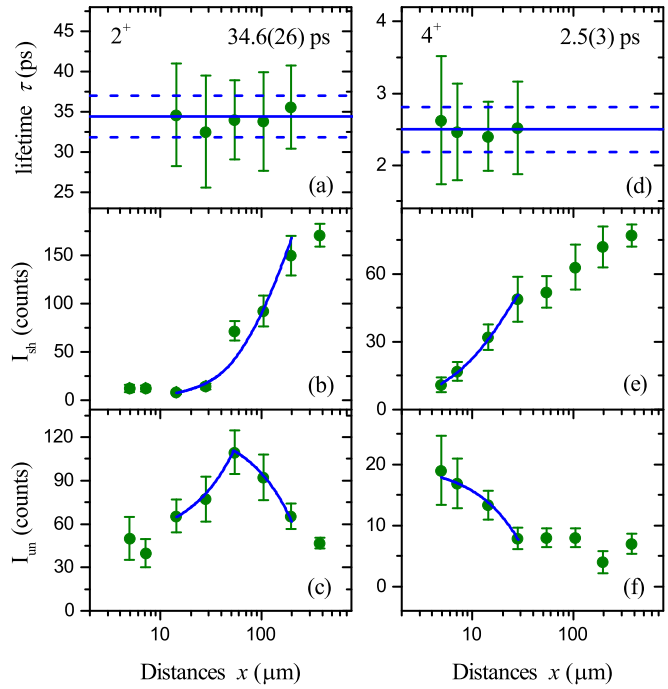

FIG. 3. Lifetime values $\tau(x)$ and their average values for the $2_1^+ \rightarrow 0_1^+$ transition at 409.1 keV (a) and $4_1^+ \rightarrow 2_1^+$ transition (d) at 639.7 keV, measured by the detectors at backward angular ($\theta = 153^\circ$). The associated intensities of the shifted [(b) and (e)] and unshifted [(c) and (f)] components are also shown.

from the 10_1^+ level at 3207.9 keV. The known isomeric 10_1^+ state at 3207.9 keV has a lifetime of $\tau = 444$ ns and therefore has no influence on the present prompt lifetime measurement. In contrast to this slow feeding, the expected lifetimes of the low-lying levels in the ground-state band in ^{134}Ce are of the order of a few or tens ps. The long-lived 5^- state at 2174.0 keV would result in a mass of Doppler shifted intensity missing for analysis of 2_1^+ and 4_1^+ states. The other two long lifetimes of the 10_2^+ and 12_2^+ states also lead to a relatively long effective feeding time for the low-lying levels. The similar consequence could have been the missing shift for levels populated by these states, particularly for much shorter-lived levels. The existence of the above mentioned long-lived states would not affect the analysis of the lower-lying levels when using the DDCM in coincidence mode, but greatly reduced the statistics of the lower-lying levels especially when they were fed dominantly. Because of this effect, in the present experiment, only enough statistics were collected to allow gating on the shifted component of the feeding transition for determination the lifetimes of 2_1^+ and 4_1^+ states in the ground band.

The lifetime of the 2_1^+ state at 409.1 keV was determined through a direct gate on the Doppler-shifted component of the 639.7 keV, $4_1^+ \rightarrow 2_1^+$ transition. The occurrence of the 644.6 keV, $5^+ \rightarrow 3^+$ transition prevented placing a gate on the forward (42°) shifted component of the populating transition. Examples of gated spectra for different target-to-stopper distances at backward angular 153° are given in Fig. 1. The results of the analysis according to DDCM at backward angle are shown in Fig. 3. The bottom panel [Fig. 3(c)] illustrates the variation of the normalized intensities of the unshifted components of the 409.1 keV transition as a function of distances x corresponding to the denominator of Eq. (1). The intensity of the shifted peak is illustrated in the middle panel [Fig. 3(b)]. The weighted mean of the lifetimes $\tau = 34.6(26)$ ps for 2_1^+ state are shown in Fig. 3(a). The range of distances used for evaluating the mean τ is limited to the sensitive region of the measurement, where the numerator and denominator of Eq. (1) are not close to zero. The lifetime curves obtained for forward angle were also obtained, yielding $\tau = 32.9(29)$ ps, showing consistent agreement. Finally, the result for the lifetime of the 2_1^+ state is adopted as the average of these two values: $\tau = 33.8(28)$ ps, which is consistent within error with the previous measurement [7] of 32.7(28) ps.

The 4_1^+ level is mainly populated by the 814.5 keV, $6_1^+ \rightarrow 4_1^+$ transition and 1125.2 keV, $5_1^- \rightarrow 4_1^+$ transition, and depopulated by the 639.7 keV transition. Because of the long lifetime of the 5_1^- level, only interband cascade could be used for the gating analysis. At forward angles, the shifted component of the direct feeding 814.5 keV transition cannot be separated from the contamination by the 817.2 keV $16^+ \rightarrow 14^+$ transition, which means that the forward detectors could also not be used for gating. However, in the spectra obtained from the backward detectors, there is still partial

TABLE I. Experimentally measured lifetime values τ and calculated $E2$ transitions strengths for excited states in ^{134}Ce measured in this work.

E_γ (keV)	$J_i \to J_f$	τ (ps)		$B(E2)$ (W.u.)
		Present	Previous[a]	
409.1	$2_1^+ \to 0_1^+$	33.8(26)	32.7(28)	50.8(41)
639.7	$4_1^+ \to 2_1^+$	2.4(3)	4.5(8)	77.6(97)
907.8	$10_2^+ \to 8_1^+$	9.6(9)	8.6(14)	3.8(3)
464.1	$12_2^+ \to 10_2^+$	16.7(15)	15.9(19)	54.9(49)

[a]Data are taken from Ref. [7].

overlap between the shifted component of the 814.5 keV transition and the shifted component of contamination by the 817.2 keV transition. As a result, only a narrow gate width on the faster-velocity tail is used; furthermore, the velocity v of the recoils is determined by the gating region, e.g., $v/c = 1.02\%$ for extraction of the lifetimes of 4_1^+ state. A small unshifted part of the 639.7 keV ($4_1^+ \to 2_1^+$) γ ray and no unshifted part of the 814.5 KeV ($6_1^+ \to 4_1^+$) and 947.8 KeV ($8_1^+ \to 6_1^+$) γ rays were observed for target-to-stopper distances larger than 8 μm with gates on the shifted component of their directly feeding transitions, which indicate short lifetimes of 4_1^+, 6_1^+, and 8_1^+ states. It should be noted that about 50% feeding of the ground state band is from relatively long-lived 10_2^+ and 12_2^+ states. The γ-ray in-flight emission from these two states will continuously contribute to the observation of both of the Doppler shifted and unshifted γ rays of ground states. Thus, the Doppler-shifted component the of directly feeding transition (814.5 keV, $6_1^+ \to 4_1^+$) will increase as the distance increases until the shifted component reaches a constant level at a larger distance, which is out of the sensitive range of the 10_2^+, 12_2^+ states; accordingly, the Doppler-shifted component of the transition (639.7 keV, $4_1^+ \to 2_1^+$) will also increase as the distance increases, as shown in Fig. 3(e). At the same time, the intensities of the unshifted peak did not rapidly vanish [shown in Fig. 3(f)], but were a constant small value for target-to-stopper distances larger than 28 μm, which is intuitively out of the sensitive range of the ($4_1^+ \to 2_1^+$) transition. The final lifetime results for each of the used gradients at four target-to-stopper distances x are given in the upper panel of Fig. 3 (right). It can be seen what the value obtained is practically constant with the distance, indicating that there is no problem with slow feeding into the 4_1^+ state. The lifetimes obtained for both forward and backward angles show consistent agreement with an average of $\tau = 2.4(3)$ ps, which is about two times smaller than the previously known result.

Similar spectra analysis were performed in order to determine the lifetimes of the 10_2^+ and 12_2^+ states, in which the gates on the direct feeding transition could be employed without problems from contamination. Due to poor statistics or limited distance in the present experiment, levels at higher excitation energies and negative parity-band could not be analyzed. The four lifetimes measured in this work and the corresponding $B(E2)$ values expressed in single-particle Weisskopf units (W.u.) are summarized in Table I.

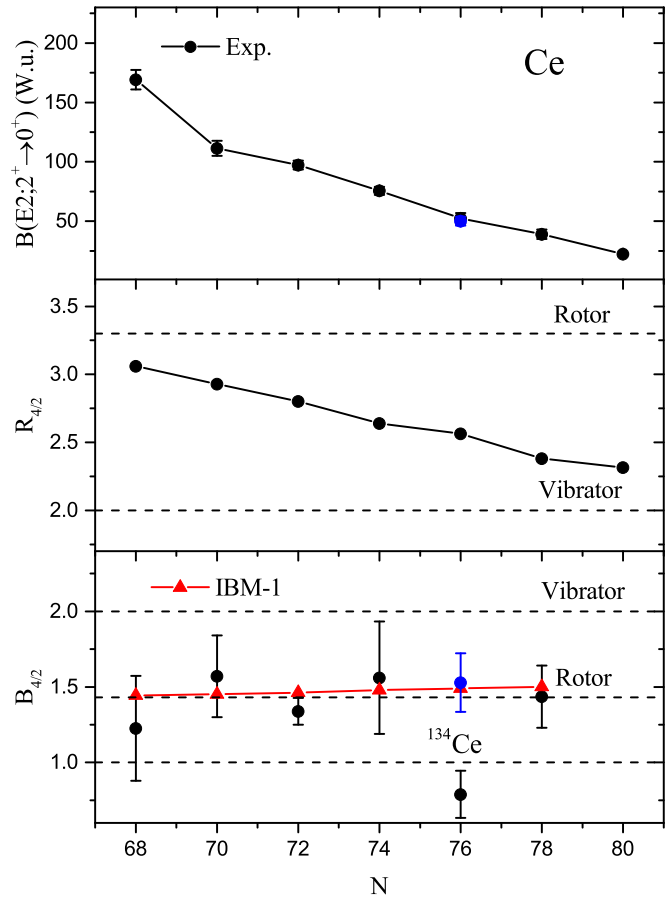

FIG. 4. Top: the systematic of the $B(E2; 2_1^+ \to 0_1^+)$ value in cerium isotopes. Middle: the systematic of the $R_{4/2}$ value in cerium isotopes. Bottom: the systematic of the $B_{4/2}$ value in cerium isotopes compared to the IBM-1 calculations. Data are taken from Refs. [7,18–21] and filled circles (blue) correspond to values measured in the present work.

IV. DISCUSSION

As mentioned above, the lifetime of the 2_1^+ level in ^{134}Ce is inconsistent with the previous value. However, the lifetime of the 4_1^+ level is about two times smaller than the previously known result. Thus, the new value for the $B_{4/2}$ ratio is 1.53(19), which removes ^{134}Ce from the list of possible anomalies identified in Ref. [2] for now. The systematics of the $B(E2; 2_1^+ \to 0_1^+)$, $R_{4/2}$, and $B_{4/2}$ values are shown for the even-even $^{126-136}$Ce isotopes in Figs. 4(a), 4(b), and 4(c). The determined $B(E2; 2_1^+ \to 0_1^+)$ value in this work fits nicely into a smoothly developing systematics expected by a simple valence nucleon picture, and the downward trend reflects the reduced collective character going toward closed shell. The excitation energy $R_{4/2}$ ratios also show a smooth development from a rotor structure toward a vibrational structure when approaching closed shell. A value of the energy ratio $R_{4/2} = 2.56$ is obtained for ^{134}Ce, positioned with $N = 76$ approaching closed shell $N = 82$. This is close to the typical value for an ideal γ-soft rotor or a nucleus that can be described with the dynamical symmetry O(6) of the interacting boson model (IBM).

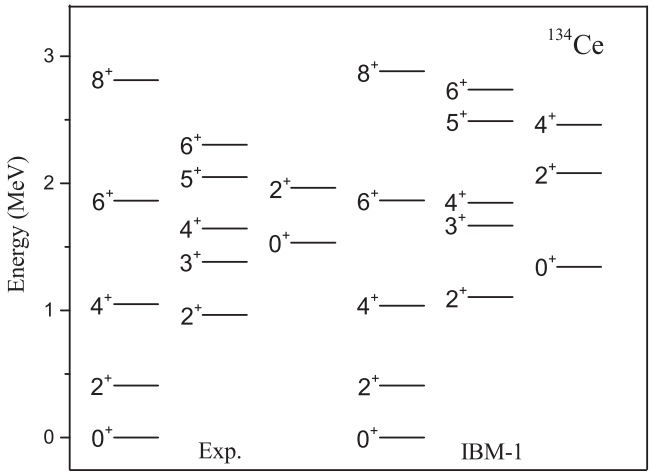

FIG. 5. Experimental level energies for ^{134}Ce compared with IBM-1 calculations. Energies are normalized to the experimental $E(2_1^+)$ value.

Additionally, the new $B_{4/2}$ value in ^{134}Ce also fits into the systematics, which are close to the Alaga value of 10/7 [22], clearly exhibiting rotational structure. However, special physics effects, e.g., single-particle structural influence due to the closing of the proton $g_{7/2}$ orbital, resulting in a subshell closure at $Z = 58$, have been considered for heavier ^{136,138}Ce nuclei in the study of the fragmentation of the one-phonon mixed-symmetry 2^+ excitation [23,24]. The new measurement $B_{4/2}$ in ^{134}Ce conforms to the collective nature and there is no indication of any deviation from the general trend of evolution, in contrast to what is indicated by the $B(E2; 2_1^+ \rightarrow 0_1^+)$ and $R_{4/2}$ values.

To understand the collectivity of ^{134}Ce, we employed the interacting boson model (IBM) [25,26], which is successful in describing low-lying collective states in many even-even nuclei. The evolution of collectivity across the neutron-deficient Ce isotopic chain has recently been used to examine in detail systematics employing the IBM-1 [27,28]. The excitation energies of the lowest positive-parity levels in the Ce isotopes and a limited set of electromagnetic transition rates for these nuclei were investigated in each of these studies, as well as two-neutron separation energies in Ref. [27]. The model parameters obtained were mapped onto the IBM symmetry triangle in Ref. [27] to show that ^{134}Ce was best described within the intermediate parameter, deviating somewhat toward SU(3) from the line interconnecting U(5) and O(6).

In Fig. 5 we show the low-spin spectra of ^{134}Ce compared to those calculations within IBM-1 using the parameters of Ref. [27]. It was found in their work that the addition of the octupole term in the IBM-1 Hamiltonian plays an important role in reproducing the properties of the low-lying collective states. Thus, the Hamiltonian employed in the present work was the same as the one used in Ref. [27] including the octupole term. The calculations provide a good description of the low-lying spectra for a wide range of structures. The partial discrepancy in reproducing the staggering of the γ band and the spacing of the $K = 0$ band is a well-known issue [29,30].

For electromagnetic transition rates, due to the predictive power of the IBM, is limited by relying on the effective charges. Therefore, the $B_{4/2}$ ratio, which is independent of the effective charge, is used to judge the predictions of the IBM-1 calculations. $B_{4/2}$ is 2.0 in a pure geometric vibrator and about 1.5 in the finite particle IBM model. It is 1.43 in a pure rotor. As mentioned above, for ^{134}Ce, the remeasured $B_{4/2}$ value is 1.53(19), which is in good agreement with the IBM-1 calculated one of $B_{4/2} = 1.49$.

Furthermore, the systematics of $B_{4/2}$ values of IBM-1 calculations are also presented in Fig. 4(c). As can be seen in the figure, the ratio and its trend of being fairly constant over the considered range of nuclei is reproduced well within the IBM-1. It is concluded in Ref. [27] that the neutron-deficient nuclei show many features associated with a triaxial γ-soft rotor, represented by the O(6) symmetry, but approach a spherical structure, the U(5) symmetry, with increasing neutron number toward the $N = 82$ shell closure. As can be seen in Fig. 4(c), the $B_{4/2}$ values follow a general trend like that of the calculations in the IBM-1 model. In the earlier work on the algebraic model, the IBM-2 was applied to the study of shape phase transition of $^{128-138}$Ce isotopes [31]. Their use of a complete Hamiltonian shows that γ-soft rotor features exist in Ce, but with a dominance of vibrational character. The $B_{4/2}$ increases from about 1.40 for $N = 70$ to 1.50 for $N = 80$, which is also in good agreement with the experimental value. As the main focus of this work was the determination of the $B_{4/2}$ value, further lifetime measurements to delineate the yrast band structures to higher spin and the non-yrast band are required to gain a full understanding of all the features in Ce isotopes.

V. SUMMARY

In summary, new lifetime measurements of the 2_1^+, 4_1^+, 10_2^+, and 12_2^+ states in ^{134}Ce have been performed using the recoil distance method. The measured lifetimes of the 2_1^+, 10_2^+, and 12_2^+ states from this experiment are in agreement with previous measurements. In the case of the 4_1^+ state, the values obtained in the present work contradict previous measurements, from which the newly determined lifetime is about two times smaller than the previous value, and resolve the disagreement in the published lifetimes of the 4_1^+ state that were subject to discussions in the literature due to a $B_{4/2}$ value smaller than unity. The present experimental study suggests that, like most of the atomic nuclei, the nature of the low-lying excitation in ^{134}Ce does not present subshell or shell closure character, but is a transitional nucleus with a ratio $B_{4/2}$ larger than 1. Predictions based on the interacting boson model yield good agreement with the new measurement presented in the present paper and the systematics along the Ce isotopical chains.

ACKNOWLEDGMENTS

The authors wish to thank the HI-13 tandem accelerator staff for the smooth operation of the machine. The authors would like to thank S. Pascu for his providing the detailed

parameters of IBM model. The authors are grateful to Dr. Q. W. Fan for his assistance during target preparation. This work is partially supported by the National Natural Science Foundation of China under Contracts No. 11405274, No. 11075214, No. 11375267, No. 11305269, No. 11475072, and No. 11175259.

[1] J. J. Ressler, R. F. Casten, N. V. Zamfir, C. W. Beausang, R. B. Cakirli, H. Ai, H. Amro, M. A. Caprio, A. A. Hecht, A. Heinz, S. D. Langdown, E. A. McCutchan, D. A. Meyer, C. Plettner, P. H. Regan, M. J. S. Sciacchitano, and A. D. Yamamoto, Phys. Rev. C **69**, 034317 (2004).
[2] R. B. Cakirli, R. F. Casten, J. Jolie, and N. Warr, Phys. Rev. C **70**, 047302 (2004).
[3] D. Radeck, V. Werner, G. Ilie, N. Cooper, V. Anagnostatou, T. Ahn, L. Bettermann, R. J. Casperson, R. Chevrier, A. Heinz, J. Jolie, D. McCarthy, M. K. Smith, and E. Williams, Phys. Rev. C **85**, 014301 (2012).
[4] E. Williams, C. Plettner, E. A. McCutchan *et al.*, Phys. Rev. C **74**, 024302 (2006).
[5] O. Möller, N. Warr, J. Jolie, A. Dewald *et al.*, Phys. Rev. C **71**, 064324 (2005).
[6] C. R. Fitzpatrick, V. Werner, R. F. Casten *et al.*, Phys. Rev. C **78**, 034309 (2008).
[7] D. Husar, J. S. Mills, H. Craf, U. Neumann, and D. Pelte, Phys. Rev. Lett. **36**, 1291 (1976).
[8] T. K. Alexander and J. S. Forster, Adv. Nucl. Phys. **10**, 197 (1978).
[9] A. Dewald, O. Möller, and P. Petkov, Prog. Part. Nucl. Phys. **67**, 786 (2012).
[10] A. Dewald, S. Harissopoulos, and P. von Brentano, Z. Phys. A **334**, 163 (1989).
[11] G. Böhm, A. Dewald, P. Petkov, and P. von Brentano, Nucl. Instrum. Methods Phys. Res., Sect. A **329**, 248 (1993).
[12] Q. M. Chen, X. G. Wu, Y. S. Chen, C. B. Li, Z. C. Gao, G. S. Li, F. Q. Chen, C. Y. He, Y. Zheng, S. P. Hu, J. Zhong, Y. H. Wu, H. W. Li, and P. W. Luo, Phys. Rev. C **93**, 044310 (2016).
[13] C. M. Petrache, S. Guo, A. D. Ayangeakaa, U. Garg, J. T. Matta, B. K. Nayak, D. Patel, M. P. Carpenter, C. J. Chiara, R. V. F. Janssens, F. G. Kondev, T. Lauritsen, D. Seweryniak, S. Zhu, S. S. Ghugre, and R. Palit, Phys. Rev. C **93**, 064305 (2016).
[14] M. Moller-veggian, H. Beuscher, D. R. Haenni, R. M. Lieder, and A. Neskakis, Nucl. Phys. A **417**, 189 (1984).
[15] T. Alharbi, P. H. Regan, N. Marginean, Zs. Podolyak, O. J. Roberts, A. M. Bruce, N. Alkhomashi, R. Britton, D. Bucurescu, D. Deleanu, D. Filipescu, D. Ghita, T. Glodariu, C. Mihai, K. Mulholland, R. Lica, R. Marginean, M. Nakhostin, A. Negret, C. R. Nita, L. Stroe, T. Sava, C. Townsley, and N. V. Zamfir, Phys. Rev. C **91**, 027302 (2015).
[16] T. Alharbi, P. H. Regan, N. Marginean *et al.*, Phys. Rev. C **87**, 014323 (2013).
[17] E. Dafni, F. D. Davidovsky, A. Gelberg, M. Haas, E. Naim, and G. Schatz, Hyperfine Interact. **15**, 101 (1983).
[18] A. Makishima, T. Ishii, M. Ogawa, and M. Ishii, Nucl. Instrum. Methods Phys. Res. A **363**, 591 (1995).
[19] R. Moscrop, M. Campbell, W. Gelletly *et al.*, Nucl. Phys. A **481**, 559 (1988).
[20] T. Klemme, A. Fitzler, A. Dewald *et al.*, Phys. Rev. C **60**, 034301 (1999).
[21] F. Naqvi, V. Werner, P. Petkov, T. Ahn, N. Cooper, G. Ilie, D. Radeck, C. Bernards, M. P. Carpenter, C. J. Chiara, R. V. F. Janssens, F. G. Kondev, T. Lauritsen, D. Seweryniak, Ch. Stoyanov, and S. Zhu, Phys. Lett. B **728**, 303 (2014).
[22] G. Alaga, K. Adler, A. Bohr, and B. R. Mottelson, Mat. Fys. Medd. K. Dan. Vidensk. Selsk. **29**, 9 (1955).
[23] T. Ahn, G. Rainovski, N. Pietralla, L. Coquard, T. Möller, A. Costin, R. V. F. Janssens, C. J. Lister, M. P. Carpenter, and S. Zhu, Phys. Rev. C **86**, 014303 (2012).
[24] G. Rainovski, N. Pietralla, T. Ahn, C. J. Lister, R. V. F. Janssens, M. P. Carpenter, S. Zhu, and C. J. Barton III, Phys. Rev. Lett. **96**, 122501 (2006).
[25] R. F. Casten and D. D. Warner, Rev. Mod. Phys. **60**, 389 (1988).
[26] A. Arima and F. Iachello, Phys. Rev. Lett. **35**, 1069 (1975).
[27] S. Pascu, N. V. Zamfir, Gh. Căta-Danil, and N. Mărginean, Phys. Rev. C **81**, 054321 (2010).
[28] J. B. Gupta and Krishna Kumar, Nucl. Phys. A **882**, 21 (2012).
[29] N. V. Zamfir and R. F. Casten, Phys. Lett. B **260**, 265 (1991).
[30] G. Gneuss and W. Greiner, Nucl. Phys. A **171**, 449 (1971).
[31] N. Turkan and I. Maras, Pramana J. Phys. **68**, 769 (2007).